

P.R. ŻABIŃSKI*, R. KOWALIK*, M. PIWOWARCZYK*

COBALT-TUNGSTEN ALLOYS FOR HYDROGEN EVOLUTION IN HOT 8 M NaOH

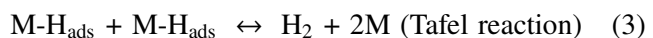
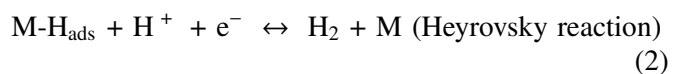
WYDZIELANIE WODORU W GORĄCYM 8 M NaOH NA STOPACH KOBALT-WOLFRAM

Tailoring of active cobalt alloy cathodes for hydrogen evolution in a hot concentrated sodium hydroxide solution was attempted by electrodeposition. Enhancement of cathodic activity of cobalt for electrolytic hydrogen evolution has been carried out by the formation of Co-W-C alloys containing different contents of tungsten. The carbon addition to Co-W alloys was made to enhance the electrolytic hydrogen evolution activity and to prevent open circuit corrosion in 8 M NaOH at 90°C. The best condition for electrodeposition of Co-W-C alloy was pH 4, the $\text{CoSO}_4 \cdot 7\text{H}_2\text{O}$ concentration of 30 g/l, the $\text{NaWO}_4 \cdot 2\text{H}_2\text{O}$ concentration of 20 g/l and arginine concentrations of 0.005–0.05 M. Under this condition the alloy was composed of an amorphous phase and showed high hydrogen evolution activity. The carbon addition was effective in enhancing the hydrogen evolution activity and in preventing dealloying due to preferential dissolution of tungsten during open circuit immersion in the hot alkaline solution.

Na drodze elektrolizy otrzymywano stopy kobaltowe o wysokiej aktywności w procesie wydzielania wodoru w gorącym stężonym roztworze wodorotlenku sodu. Poprawa aktywności kobaltu w procesie elektrolytycznego wydzielania wodoru została dokonana poprzez osadzanie stopów Co-W-C zawierających różne zawartości wolframu. Dodatek węgla do stopów Co-W powodował poprawę aktywności stopu w procesie wydzielania wodoru oraz zapobiegał korozji stopu w 8 M NaOH w temperaturze 90°C. Najlepsze warunki osadzania stopów Co-W-C to pH 4, 30 g/l $\text{CoSO}_4 \cdot 7\text{H}_2\text{O}$, 20 g/l $\text{NaWO}_4 \cdot 2\text{H}_2\text{O}$ oraz 0.005–0.05 M argininy. W tych warunkach stopy wykazywały strukturę amorficzną i miały najwyższą aktywność w procesie wydzielania wodoru. Dodatek węgla w stopie był skuteczny w poprawie aktywności stopu w procesie wydzielania wodoru oraz zapobiegał selektywnemu roztwarzaniu wolframu w gorącym roztworze alkalicznym.

1. Introduction

Hydrogen is increasingly considered as the fuel of the future [1–4]. The production of hydrogen by water electrolysis represents a process where hydrogen can be produced by true renewable and fully environmentally friendly energy sources, without evolution of the green-house gas, CO_2 . Industrial water electrolysis is, for the time being, carried out using alkaline electrolyte. The disadvantages of this technology are mainly related to low specific production rates, high energy consumption, low efficiency, voluminous systems, and safety issues related to use of caustic electrolytes. The hydrogen evolution reaction (HER) on a metallic electrode M, proceeds according to the three-reaction mechanism [5]:



These reactions are usually referred to as the charge transfer (discharge) or Volmer reaction, Reaction 1, the electrochemical desorption (ion-atom recombination) or Heyrovsky reaction, Reaction 2, and the atom-atom recombination or Tafel reaction, Reaction 3. M here represents the free metal surface (e.g., Ni), and M-H_{ads} the atomic hydrogen adsorbed on the metal surface. In this mechanism, Reaction 1 is followed by an electrochemical reaction (2), or a chemical desorption reaction (3) step. For metals that are good catalysts toward HER, the Tafel reaction is the rate-determining step (rds) at low overpotentials, while at higher overpotentials, the Heyrovsky reaction becomes the rds. At large overpotentials,

* FACULTY OF NON-FERROUS METALS, AGH UNIVERSITY OF SCIENCE AND TECHNOLOGY, 30-059 KRAKÓW, 30 MICKIEWICZA AVE., POLAND

the Volmer reaction becomes the rds due to surface coverage by adsorbed H [6].

Research in the area of HER catalyst development has been mainly focused on several areas of interest: (i) intrinsic nature of the reaction [7–10], (ii) electrode composition [11–15], (iii) surface morphology [7–9, 15–20], (iv) structural, chemical and electronic properties [11–14, 21], and (v) physical, chemical and electrochemical activation treatments [7–9, 22–23]. Two properties play an important role in selecting catalytically active materials for the HER: the actual electrocatalytic effect of the material, which is directly dependent on the overpotential used to operate the electrolytic cell at significant current densities and the catalyst stability. A desired decrease in overpotential can be achieved by choosing an electrode material of high intrinsic catalytic activity for the HER and/or by increasing the active surface area of the electrode.

With respect to the enhancement of the electrocatalytic activity by increasing the active surface area of the electrode, Ni-based alloys have been successfully used to fabricate HER cathodes in classical alkaline electrolytic cell [8, 9, 20, 23]. Enhancement of cathodic activity of nickel for electrolytic hydrogen evolution has been carried out by the formation of nickel alloys such as Ni-S [24], Raney Ni [25], Ni-Mo [26–32], Raney Ni-RuO [25, 33], Ni-Sn [34], Ni-Mo-O [35, 36] and Ni-Fe-C [37, 38]. Among them, electrodeposited Ni-Fe-C alloys have shown the highest activity for hydrogen evolution in hot alkaline solutions and excellent durability: The overpotential for hydrogen evolution at the current density of 1000 Am^{-2} in 8 M NaOH at 90°C was less than 100 mV. The activity did not decrease and no iron dissolution occurred during open circuit immersion in the hot alkaline solution.

The activity of cobalt for hydrogen evolution is comparable to that of nickel, and hence there would be a possibility for cobalt to be active electrodes for hydrogen evolution by proper alloying [39, 40]. It has been known that dealloying corrosion due to preferential dissolution of molybdenum and iron in the form of oxyanions from Ni-Mo and Ni-Fe alloys occurs during open circuit immersion in hot alkaline solutions. As has been found for Ni-Mo-O [35, 36] and Ni-Fe-C [37] alloys, the additions of electronegative elements such as oxygen and carbon are quite effective in preventing the preferential dissolution of molybdenum and iron. Carbon addition to electrodeposited Co-Mo [38] and Co-Fe [39] alloys was made to enhance the electrolytic hydrogen evolution activity and to prevent open circuit corrosion in 8 M NaOH at 90°C. The addition of carbon to electrodeposited Co-Mo alloys enhanced the hydrogen evolution activity and slowed down dissolution of molybdenum during

open circuit immersion, although complete prevention of dissolution of molybdenum was not attained.

There is increasing interest in the investigation of amorphous alloys of W with iron group metals. These alloys exhibit useful properties such as high corrosion resistance and premium hardness. Additionally, the Ni-W alloy is also seen as an environmentally safe substitute for hard chromium plating and a new material for microelectronic and microelectromechanical systems and ultralarge-scale integrated systems [40].

The present work aims to obtain the Co-W and Co-W-C alloys with high cathodic activity and durability for hydrogen evolution by electrodeposition. Particular attention was paid to the effect of tungsten and carbon additions in enhancing the activity and durability for hydrogen evolution in a hot alkaline solution.

2. Experimental

The basic electrolyte used for electrodeposition was an aqueous solution consisting of 30 g/l $\text{CoSO}_4 \cdot 7\text{H}_2\text{O}$, 3.5 g/l $\text{CoCl}_2 \cdot 6\text{H}_2\text{O}$, 6.5 g/l boric acid, 23.3 g/l $\text{MgSO}_4 \cdot 7\text{H}_2\text{O}$, 0.08 g/l sodium lauryl sulfate, 1 g/l saccharin and 150 g/l citric acid monohydrate, to which 0–25 g/l $\text{NaWO}_4 \cdot 2\text{H}_2\text{O}$ was added. The addition of 0.001–0.100 M arginine to the electrodeposition solution as a carbon source was attempted for preparation of Co-W-C alloys. The pH of the electrodeposition solution was adjusted to 4 by addition of concentrated H_2SO_4 .

The substrate for electrodeposition was copper metal of 10 mm x 10 mm x 0.1 mm, at a corner of which copper wire of 1 mm diameter was spot-welded for power supply. The dimensions of cells used for electrodeposition were 40 mm wide, 100 mm long and 45 mm high. Two platinum metal anodes of 0.1 mm thickness were placed vertically at both ends of the cell, facing each other with distance of about 93 mm. The surface of the anodes facing to the inside of the cell was 4 cm^2 . The substrate was placed vertically in the center of the cell and parallel to the anodes. The substrates were chemically etched in the $\text{HNO}_3 : \text{CH}_3\text{COOH} : \text{H}_2\text{PHO}_3$ 1:1:1 mixture for 10 s at temperature 60°C. According to preliminary experiments, agitation of the deposition electrolyte did not affect definitely the composition and hydrogen evolution performance of the deposits because of violent hydrogen evolution during electrodeposition, and hence electrodeposition was carried out under a stagnant condition at 25°C and a current density of 400 Am^{-2} for 1 hour.

The surface morphology and composition of elements in the electrodes thus prepared was analyzed by using of scanning microscopy Philips XL30 equipped with EDS analyzer and carbon was chemically analyzed

by combustion infrared absorption method. For carbon analysis thick alloys were prepared on mechanically polished substrate by deposition for 24 hours. The deposits were peeled off from the substrates and used for carbon analysis.

Subtle changes in modified surface layer of samples were examined using the X-ray Photoelectron Spectroscopy. XPS studies give surface information about the few uppermost nanometers of a sample. Therefore Auger microprobe analyzer, Microlab 350 (Thermo Electron) was applied in order to monitor surface morphology and local chemical composition, utilizing the XPS functions of the Microlab with a lateral resolution of several mm for XPS. The chemical state of surface species was identified using the XPS spectrometer (the energy resolution of the spherical sector analyzer is continuously variable between 0.6% and 0.06%). The appropriate standards for XPS reference spectra were also used. XPS spectra were excited using Al K α ($h\nu = 1486.6\text{eV}$) radiation as a source. The measured binding energies were corrected referring to energy of C1s in 285eV. An Avantage based data system was used for data acquisition and processing.

The current efficiency for electrodeposition was estimated from the mass of the deposit and the charge passed the cell measured by means of coulometer. The structure of the electrodes was identified by X-ray diffraction using Cu K α radiation. The grain size of the deposits was estimated from the full width at half maximum of the most intense diffraction line by Scherrer's equation [41].

The hydrogen evolution activity of the electrodes was examined in 8 M NaOH solution at 90°C by galvanostatic polarization. A cell of acrylic resin with the specimen electrode, a platinum counter electrode and an external calomel reference electrode having a reversible potential of 1.05V for the hydrogen reaction was used. The ohmic drop was corrected using a current interruption method.

3. Results and Discussion

Tailoring of active and durable cobalt-tungsten alloy cathodes for hydrogen evolution in hot concentrated sodium hydroxide solution was attempted by electrodeposition. Table 1 shows the change in binary Co-W alloy composition with sodium tungstate concentration of the solution for electrodeposition. Increasing tungsten salt concentration in the solution leads to an increase in tungsten content in deposit. The codeposition of cobalt with tungsten occurs in all solutions with sodium tungstate. The maximum content of tungsten in the alloy electrodeposited from the electrolyte containing 20 g/l of NaWO₄·2H₂O was 9.8 at%. The current efficiency is low due to violent hydrogen evolution during electrode-

position. The current efficiency does not change with an increase in tungsten content in electrolyte up to 7.5 g/l of NaWO₄·2H₂O and its value is about 6% independent of electrolyte composition. The current efficiency increases with sodium tungstate content in electrolyte when its content is 10 g/l or more. The highest current efficiency is observed when sodium tungstate content in electrolyte is 25 g/l. The increase in current efficiency for alloys with higher tungsten content may be connected with change in structure deposit from fcc to hcp as shown in Figure 1.

TABLE 1
Change in composition of binary Co-W alloy deposits
with concentration of NaWO₄·2H₂O in the electrolyte at pH 4

NaWO ₄ ·2H ₂ O concentration in electrolyte [g/l]	Cobalt content of alloy [at %]	Tungsten content of alloy [at %]	Cathodic current efficiency [%]
0	100	0	6.6
2	98.5	1.5	6.6
5	95.9	4.1	6.5
7.5	94.5	5.5	6.6
10	92.4	7.6	6.9
15	92.4	7.6	8.1
20	91.2	9.8	7.4
25	91.7	9.3	10.6

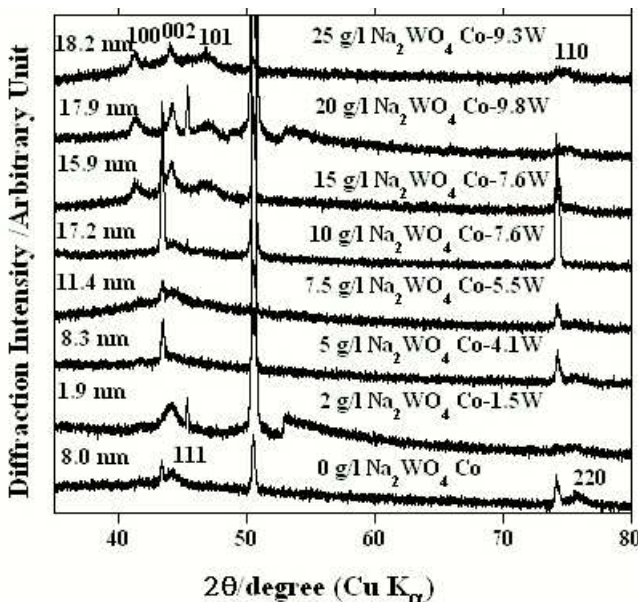


Fig. 1. X-ray diffraction patterns of Co-W alloys prepared at different concentrations of Na₂WO₄·2H₂O in the electrolyte at pH 4

Figure 1 shows X-ray diffraction patterns of binary Co-W deposits and cobalt metal deposit. The reflections at about 43.3, 50.5 and 74.2 degrees arise from the fcc copper substrate with the 100 preferred orientation.

According to X-ray diffraction patterns, alloys with low tungsten contents were composed of the nanocrystalline fcc phase. Increasing $\text{Na}_2\text{WO}_4 \cdot 2\text{H}_2\text{O}$ in the solution to 15 g/l resulted in change of crystalline structure of the deposit to the nanocrystalline hcp phase by containing 7.6 at% of W. The apparent grain sizes estimated from the full width at half maximum of the 111 reflection for deposit with fcc structure and the 002 reflection for deposits with hcp structure were written in the figure. Estimated grain size for deposited cobalt metal is 8.0 nm. The deposition of the fcc alloy with a content of tungsten, 7.6 at%, leads to grain coarsening and estimated grain size is 17.2 nm.

The further increasing of $\text{Na}_2\text{WO}_4 \cdot 2\text{H}_2\text{O}$ in electrolyte over 10 g/l results in deposition of the alloy with higher content of tungsten in deposit and change of the structure from cubic to hexagonal. The polycrystalline deposits from electrolyte with tungsten salt content from 15 to 25 g/l show polycrystalline hcp structure. The 20 values of reflections of the hcp phase in the top most diffraction pattern were definitely lower than those of the hcp cobalt. This fact indicates the lattice expansion by alloying with tungsten. The deposition of the alloy from electrolyte with a high content of tungsten salt, 25 g/l, leads to grain coarsening and estimated grain size is 18.2 nm for Co-9.3W alloy.

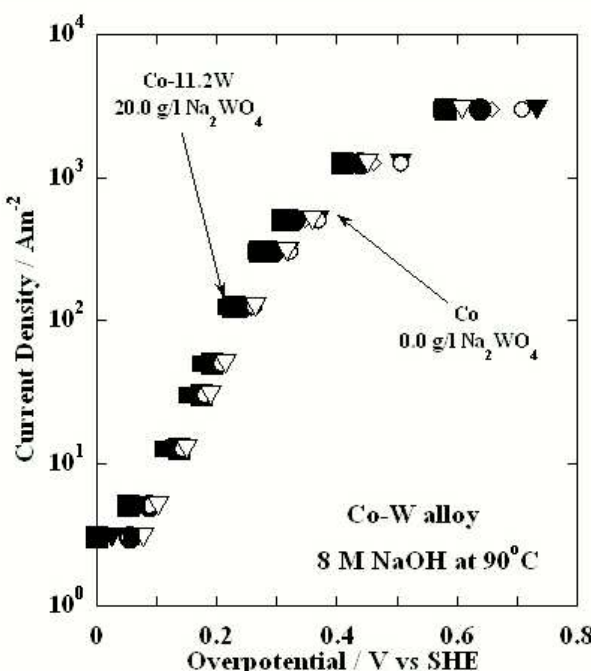


Fig. 2. Galvanostatic polarization curves for hydrogen evolution in 8 M NaON at 90°C for Co-W alloys deposited in solution at different concentration of $\text{Na}_2\text{WO}_4 \cdot 2\text{H}_2\text{O}$ in the electrolyte at pH 4

Figure 2 shows the change in the hydrogen evolution activity of binary Co-W alloys with tungsten content in solutions for electrodeposition. The Tafel slope

at lower current densities was about 145 mV/decade for cobalt metal. There is no change in slope and position of galvanostatic polarization curves with an increase in tungsten content of the binary alloys. Therefore no improvement in hydrogen evolution properties of alloy takes place. The Tafel slope value of about 145 mV/decade corresponds to $2RT/F$. Under the assumption that the hydrogen coverage θ is nearly 0 and that the transfer coefficient is 1/2, the Tafel slope indicates the rate-determining step of hydrogen evolution is the proton discharge for cobalt metal and Co-W binary alloys.

It has been known that the addition of carbon to Ni-Fe alloys prevents corrosive dissolution of iron from the Ni-Fe electrode in the hot alkaline solution during the shutdown period of electrolysis [37]. In case of Ni-Mo [38] and Co-Mo [39] alloys, the carbon addition increased the activity for hydrogen evolution and slowed down the open circuit dissolution of molybdenum. A similar effect may have been attained by the addition of carbon to Co-W alloys with a poor activity for hydrogen evolution.

Formation of Co-W-C alloys was attempted by adding arginine to the deposition electrolyte. For ternary alloy deposition the electrolyte with 20 g/l $\text{Na}_2\text{WO}_4 \cdot 2\text{H}_2\text{O}$ was chosen. The alloy with 9.8 at% tungsten, deposited from this electrolyte, contain the highest tungsten content in alloy.

TABLE 2
Change in composition of ternary Co-W-C alloy deposits from electrolyte with 20 g/l $\text{Na}_2\text{WO}_4 \cdot 2\text{H}_2\text{O}$ with concentration of arginine at pH 4

Arginine concentration in depositing solution [M]	Cobalt content of alloy [%]	Tungsten content of alloy [%]	Carbon content of alloy [%]	Cathodic current efficiency [%]
0.000	88.9	8.8	2.3	6.8
0.001	85.9	9.6	4.5	6.9
0.005	83.2	9.4	7.4	6.3
0.010	79.2	11.6	9.2	4.5
0.050	76.2	10.0	13.8	4.9
0.100	74.4	10.1	15.5	3.3

The relation between the carbon content of the alloy and concentration of tungsten and arginine in the deposition electrolyte is shown in Table 2. The alloy deposited from the solution without arginine contains 2.3 at% carbon, probably because of presence of sodium lauryl sulfate in electrolyte. The addition of arginine, even in a very small amount such as 0.001 M, leads to an increase in the carbon content to 4.5 at%. The presence of arginine in electrolyte definitely increases the carbon content in the alloy. The increase in the carbon content of the alloy results in a decrease in the cobalt content

to 74.4 at%, while the tungsten content of the alloy increased by a factor of 1.2 with addition of arginine to the deposition electrolyte. The increase in arginine concentration leads to a decrease in the cathodic current efficiency to about 3.3%.

Figure 3 shows X-ray diffraction pattern of Co-W-C alloys prepared from solutions with 20 g/l $\text{Na}_2\text{WO}_4 \cdot 2\text{H}_2\text{O}$ and with different concentrations of arginine. Sharp reflections are all due to the fcc copper substrate and the deposits formed from the solutions with arginine show a hallow pattern typical of the amorphous structure.

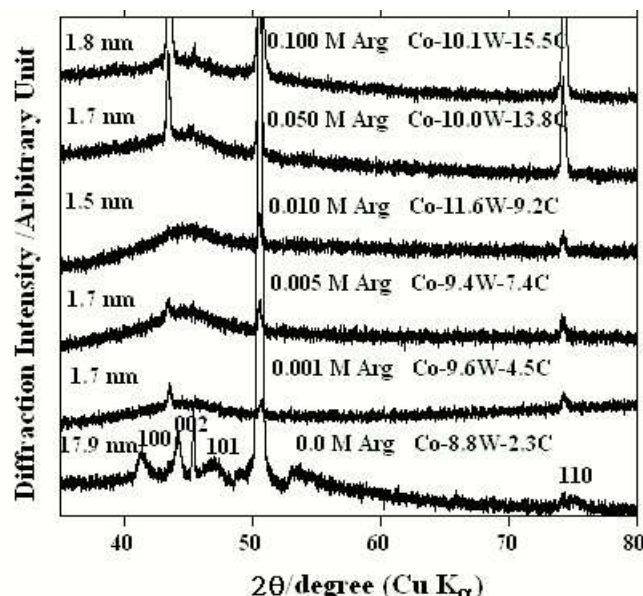


Fig. 3. X-ray diffraction patterns of Co-W-C alloys deposited in 20 g/l $\text{Na}_2\text{WO}_4 \cdot 2\text{H}_2\text{O}$ solutions with different arginine concentrations

The apparent grain sizes estimated from the full width at half maximum of the 002 reflection for deposited alloys are written in the figure. The alloys deposited from those electrolytes with sufficient high arginine content show very diffused diffraction patterns based on the hcp structure. Increasing arginine content leads to an increase in carbon content and to refining of the grain size of the deposit. The grain size of all these alloys was about 1.7 nm regardless of arginine content in comparison to 17.9 nm for alloy deposited without arginine in electrolyte. The alloys containing range of carbon such as 4–9 at% exhibit halo patterns indicating the formation of a single amorphous phase, while excess additions of carbon such as 13 at% give rise to the formation of a mixture of major amorphous and minor hcp phases.

Fig. 4 shows the change in galvanostatic polarization curves of Co-W alloys by the addition of arginine to the deposition electrolyte. The addition of arginine to the deposition electrolyte resulted in remarkable increase in the activity of the electrode; the exchange current density

increases and the Tafel slope decreases from about 145 mV/decade for the electrode prepared without arginine to about 36 mV/decade for the electrode prepared in the solution with 0.100 M arginine. The same trend of remarkable increase in the activity of electrodes has been found by the addition of carbon into Ni-Fe [37], Co-Mo [38] and Co-Fe [39] alloys prepared by electrodeposition in the solution containing lysine as the carbon source. It can, therefore, be said that the remarkable enhancement of the activity of the electrode by the addition of arginine to the deposition electrolyte seems to be due to the carbon addition to the Co-W alloys.

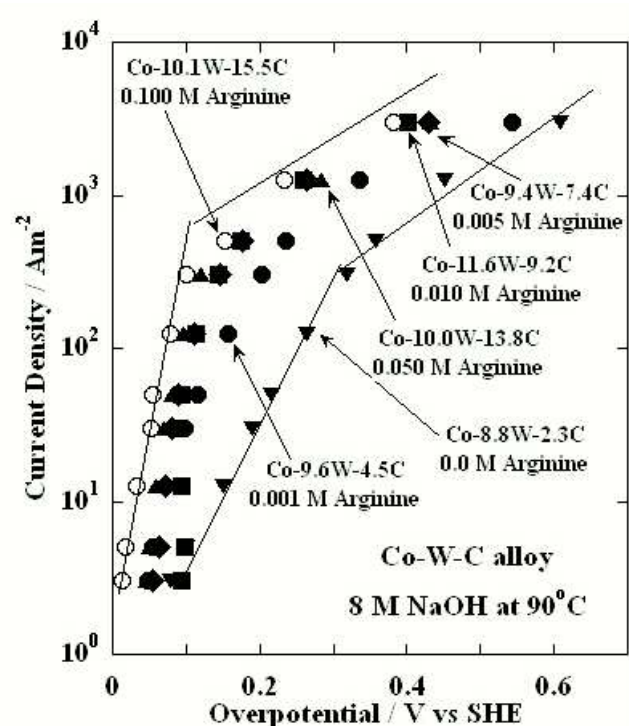


Fig. 4. Galvanostatic polarization curves for hydrogen evolution in 8 M NaON at 90°C for Co-W-C alloys deposited in 20 g/l $\text{Na}_2\text{WO}_4 \cdot 2\text{H}_2\text{O}$ solutions with different arginine concentrations

The polarization curves are composed of two regions with different Tafel slopes. An increase in arginine content in of the solution for electrodeposition remarkably enhances the hydrogen evolution activity of alloys due possibly to an increase in the carbon content of the deposits. The Tafel slope at lower current densities was about 145 mV/decade for cobalt metal but decreased to about 36 mV/decade for the Co-10.1W-8.0C alloy. These Tafel slopes correspond to 2RT/F and RT/2F for cobalt and Co-10.1W-8.0C alloy, respectively. Under the assumption that the hydrogen coverage θ is nearly 0 and that the transfer coefficient is 1/2, the change in the Tafel slope indicates the change in the rate-determining step of hydrogen evolution from the proton discharge for cobalt metal to recombination of adsorbed hydrogen for the

Co-10.1W-8.0C alloy. However, when the rate of hydrogen evolution for the Co-10.1W-8.0C alloy becomes high at higher current density, the Tafel slope again increases to about 145 mV/decade. When the proton discharge becomes significantly fast, the hydrogen coverage on the electrode surface will reach to unity and electrochemical desorption of an adsorbed hydrogen combined with a proton in the solution will be faster than the recombination of two adsorbed hydrogen atoms. When the rate determining step is electrochemical desorption of hydrogen at $\theta \approx 1$, the Tafel slope is $2RT/F$. The excess additions of carbon leads to the formation of a mixture of major amorphous and minor hcp phases, which manifest in slightly lower hydrogen evolution performance for Co-9.6W-11.1C alloy.

Very interesting from application point of view is behavior of deposited binary Co-W and ternary Co-W-C alloys during immersion in hot concentrated 8 M NaOH. The aim of this research was determining the corrosion durability of deposited alloys in open circuit conditions. It is critical point for cathodes when they are not polarized, for example during periodical shut down of installation, and hence the alloy surface is exposed to corrosive conditions.

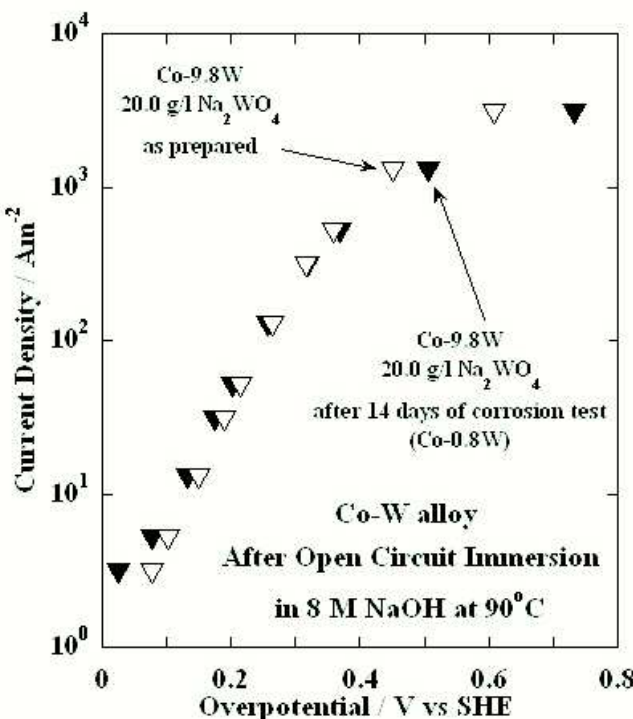


Fig. 5. Change in galvanostatic polarization curves for hydrogen evolution in 8 M NaOH at 90°C for Co-9.8W alloy with time for previous open circuit immersion in 8 M NaOH solution at 90°C for 14 days

Figure 5 shows the effect of open circuit immersion in the hot concentrated alkaline solution on the activity of the electrode for hydrogen evolution. The composi-

tions of Co-W alloys before and after 14 days of immersion test were written in the Figure. The open circuit immersion does not changes the activity for hydrogen evolution. After immersion for 14 days the Tafel slope of Co-9.8W alloy was about 145 mV/decade which is the same as that of Co-W alloy before immersion test and that of cobalt metal. The change in tungsten content of alloy by open circuit immersion in the hot concentrated alkaline solution is observed. The composition of Co-9.8W alloy after 14 days of immersion in hot concentrated alkaline solution is Co-0.8W. After immersion for 14 days almost all tungsten was dissolved into the solution. The open circuit potential which was close to the equilibrium potential for hydrogen evolution is higher than the dissolution potential of tungsten in the form of tungstate ion. Thus tungsten dissolved into the solution, whereas cobalt was in the passive state at the open circuit potential in the hot alkaline solution. A decrease in the tungsten content of the alloy surface is observed due to preferential dissolution of tungsten into the hot alkaline solution.

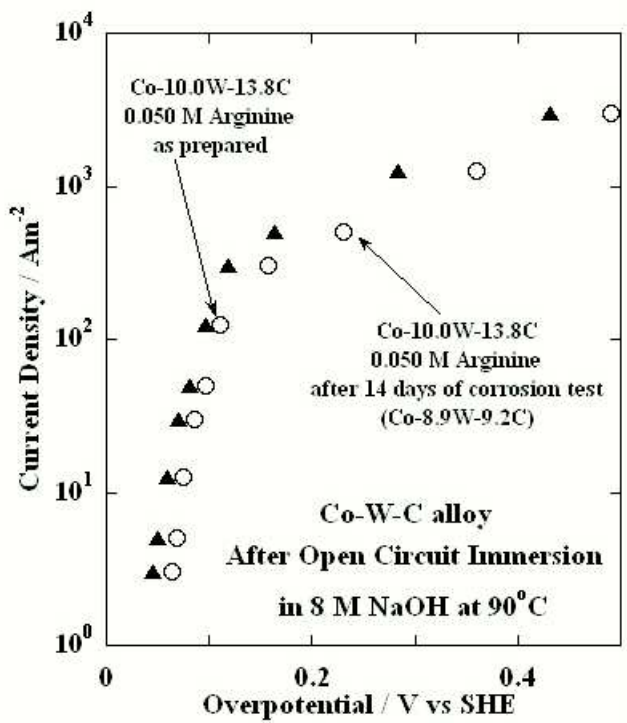


Fig. 6. Change in galvanostatic polarization curves for hydrogen evolution in 8 M NaOH at 90°C for Co-10.1W-8.0C alloy with time for previous open circuit immersion in 8 M NaOH solution at 90°C

Figure 6 shows the effect of the carbon addition on the activity for hydrogen evolution after immersion in the hot concentrated NaOH solution. While the activity of the Co-9.8W alloy for hydrogen evolution remains low, comparable to cobalt metal, with open circuit immersion, the Co-10.1W-8.0C alloy shows a high activity after im-

mersion for 14 days, although its activity is slightly lower than that of as-prepared specimen.

Although the Co-W-C alloy showed a much higher activity than the Co-W alloy after immersion for 14 days, the activity of the Co-W-C alloy for hydrogen evolution decreased by open circuit immersion. The tungsten and carbon content of Co-W-C alloys before and after open circuit immersion for 14 days were written in the Figure. Although the most of tungsten is still remaining, some tungsten was dissolved into 8 M NaOH at 90°C. This is responsible for a slightly decrease in the hydrogen evolution activity after open circuit immersion for 14 days. Thus, although the carbon addition definitely slowed down dissolution of tungsten during open circuit immersion, we regret to write that complete prevention of open circuit dissolution of tungsten in the hot alkaline solutions cannot be accomplished by the carbon addition.

On the other hand, the carbon addition increased the activity for hydrogen evolution as shown in Figure 4 and slowed down open circuit dissolution of tungsten. In order to clarify the role of carbon, X-ray photoelectron spectroscopy was performed. The change in binding energies of electrons in metals in the metallic state in the Co-W and Co-W-C alloy surfaces under the air-formed films have been analyzed. The carbon addition significantly decreases the binding energy of W 4f_{7/2} from about 32.3 eV for Co-W alloy to 31.0 eV for Co-W-C alloy. The binding energy of Co 2p_{3/2} electrons remains unchanged. This suggests the charge transfer from carbon to tungsten in the alloys. The charge transfer from carbon to tungsten may enhance the charge transfer from metal to proton, that is, proton discharge with a consequent acceleration of hydrogen evolution. The formation of bond between tungsten and carbon may also slow down dissolution of tungsten as tungstate ion. The presence of bonding between metal and carbon atoms inducing such an electronic interaction in the whole alloy surface detected by XPS may be responsible for stabilization of alloys against dealloying corrosion.

4. Conclusions

In preparation of Co-W and Co-W-C alloys by electrodeposition for hydrogen production in electrolysis of hot 8 M NaOH the following conclusions can be drawn.

The carbon addition to electrodeposited Co-W alloys was performed to enhance the activity for hydrogen evolution in 8 M NaOH at 90°C and to prevent dissolution of tungsten during open circuit immersion in the hot alkaline solution.

The best condition for electrodeposition of Co-W-C alloy was pH 4, the CoSO₄·7H₂O concentration of 30 g/l, the NaWO₄·2H₂O concentration of 20 g/l and argi-

nine concentrations of 0.005–0.05 M. Under this condition the amorphous alloy was obtained with the highest hydrogen evolution activity. When the carbon contents in the deposit were low, the Tafel slope was about 145 mV/decade, similar to cobalt metal. It suggests that the rate-determining step is proton discharge. If the carbon content of the alloys was high the activity for hydrogen evolution was much higher. For those alloys proton discharge was so fast that the rate-determining step seemed to be desorption of hydrogen from the surface of the electrode by recombination of two hydrogen atoms.

The durability of Co-W alloys for hydrogen evolution was insufficient because of dissolution of tungsten as tungstate ion during open circuit immersion in hot alkaline solutions.

In order to prevent open circuit dissolution of tungsten in the hot alkaline solution carbon addition was carried out. The carbon slowed down dissolution of tungsten from Co-W-C alloys during open circuit immersion in 8 M NaOH at 90°C, although complete prevention of open circuit dissolution was not attained.

Acknowledgements

The authors express their acknowledgment to Polish Ministry of Education and Science for financial support under grant No. 3 T08B 016 29.

REFERENCES

- [1] S. Dunn, Int. J. Hydrogen Energy **27**, 235 (2002).
- [2] T. Hijikata, Int. J. Hydrogen Energy **27**, 115 (2002).
- [3] P. Krueger, Int. J. Hydrogen Energy **25**, 395 (2000).
- [4] C. Mitsugi, A. Harumi, F. Kenzo, Int. J. Hydrogen Energy **23**, 159 (1998).
- [5] Southampton Electrochemistry Group, Instrumental Methods in Electrochemistry, Wiley, New York, 1985.
- [6] S. Trasatti, J. Electroanal. Chem. **39**, 163 (1972).
- [7] L. Chen, A. Lasia, J. Electrochem. Soc. **138**, 3321 (1991).
- [8] P. Los, A. Rami, A. Lasia, J. Appl. Electrochem. **23**, 135 (1993).
- [9] C. Hitz, A. Lasia, J. Electroanal. Chem. **500**, 213 (2001).
- [10] B.E. Conway, G. Jerkiewicz, Electrochim. Acta **45**, 4075 (2000).
- [11] J.G. Highfield, E. Claude, K. Oguro, Electrochim. Acta **44**, 2805 (1999).
- [12] H. Ezaki, M. Morinaga, S. Watanae, Electrochim. Acta **38**, 557 (1993).
- [13] H. Ezaki, M. Morinaga, S. Watanae, J. Saito, Electrochim. Acta **39**, 1769 (1994).
- [14] H. Shibutani, T. Higashijima, H. Ezaki, M. Morinaga, K. Kikuchi, Electrochim. Acta **43**, 3235 (1998).

- [15] M. Metikos-Hukovic, A. Jukic, *Electrochim. Acta* **45**, 4159 (2000).
- [16] R.K. Shervedani, A. Lasia, *J. Appl. Electrochem.* **29**, 979 (1999).
- [17] B. Losiewicz, A. Budniok, E. Rowinski, E. Łagiewka, A. Lasia, *Int. J. Hydrogen Energy* **29**, 145 (2004).
- [18] R. Simpraga, G. Tremiliosi-Filho, S.Y. Qian, B.E. Conway, *J. Electroanal. Chem.* **424**, 141 (1997).
- [19] H. Ezaki, T. Nambu, M. Morinaga, M. Ueda, K. Kawasaki, *Int. J. Hydrogen Energy* **21**, 877 (1996).
- [20] S. Tanaka, N. Hirose, T. Tanaki, *Int. J. Hydrogen Energy* **25**, 481 (2000).
- [21] M.M. Jaksic, *Electrochim. Acta* **45**, 4085 (2000).
- [22] R.K. Shervedani, A. Lasia, *J. Electrochem. Soc.* **144**, 2652 (1997).
- [23] W. Hu, *Int. J. Hydrogen Energy* **25**, 111 (2000).
- [24] H. Vanderborre, Ph. Vermeiren, R. Leyssen, *Electrochim. Acta* **29**, 97 (1984).
- [25] E. Endoh, H. Otouma, T. Morimoto, Y. Oda, *Int. J. Hydrogen Energy* **12**, 473 (1987).
- [26] J.-Y. Huot, *J. Electrochem. Soc.* **136**, 1933 (1989).
- [27] E. Belowska-Lehman, *J. Appl. Electrochem.* **20**, 132-138 (1990).
- [28] D.E. Brown, M.N. Mahmood, M.C.M. Man, A.K. Turner, *Electrochim. Acta* **29**, 1551-1556 (1984).
- [29] J.-Y. Huot, M.L. Trudeau, R. Schulz, *J. Electrochem. Soc.* **138**, 316-1321 (1991).
- [30] D. Miouesse, A. Lasia, V. Borch, *J. Appl. Electrochem.* **25**, 592-602 (1995).
- [31] A. Kawashima, E. Akiyama, H. Habazaki, K. Hashimoto, *Mater. Sci. Eng.* **A226-228**, 905-909 (1997).
- [32] C. Iwakura, N. Furukawa, M. Tanaka, *Electrochim. Acta* **37**, 757-758 (1992).
- [33] H. Yamashita, T. Yamamura, K. Yoshimoto, *J. Electrochem. Soc.* **140**, 2238-2244 (1993).
- [34] R. Schulz, J.-Y. Huot, M.L. Trudeau, L. Dingnard-Bailey, Z.H. Yan, S. Jin, A. Lamarre, E. Ghali, A. van Neste, *J. Mater. Res.* **9**, 2998-3007 (1994).
- [35] A. Kawashima, T. Sakaki, H. Habazaki, K. Hashimoto, *Mater. Sci. Eng.* **A267**, 246-253 (1999).
- [36] K. Suetsgu, T. Sakaki, K. Yoshimitsu, K. Yamaguchi, A. Kawashima, K. Hashimoto, *Chlor Alkali and Chlorate Technology: R. B. MacMullin Memorial Symposium*, H. S. Burney, N. Furuya, F. Hine and K.-I. Ota, Eds. (The Electrochemical Society 1999), 169-178.
- [37] S. Meguro, T. Sasaki, H. Katagiri, H. Habazaki, A. Kawashima, T. Sakaki, K. Asami, K. Hashimoto, *J. Electrochem. Soc.* **147**, 3003-3009 (2000).
- [38] P.R. Zabinski, H. Nemoto, S. Meguro, K. Asami, K. Hashimoto, *J. Electrochem. Soc.* **150**, C717-C722 (2003).
- [39] P.R. Zabinski, S. Meguro, K. Asami, K. Hashimoto, *Materials Transactions* **44**, 11, 1-7 (2003).
- [40] M. Donten, Z. Stojek, H. Cesulius, *J. Electrochem. Soc.* **150**, C95-C98 (2003).
- [41] P. Scherrer, *Göttingen Nachr.* **2**, 98 (1918).

Received: 10 March 2007.